ELSEVIER

Physics Letters B 543 (2002) 217–226

PHYSICS LETTERS B

www.elsevier.com/locate/npe

Transition to meson-dominated matter at RHIC. Consequences for kaon flow

L.V. Bravina [a,b], L.P. Csernai [c], Amand Faessler [a], C. Fuchs [a], E.E. Zabrodin [a,b]

[a] *Institute for Theoretical Physics, University of Tübingen, Auf der Morgenstelle 14, D-72076 Tübingen, Germany*
[b] *Institute for Nuclear Physics, Moscow State University, RU-119899 Moscow, Russia*
[c] *Department of Physics, University of Bergen, Allègaten 55, N-5007 Bergen, Norway*

Received 20 July 2001; received in revised form 25 June 2002; accepted 25 July 2002

Editor: J.-P. Blaizot

Abstract

Anisotropic flow of kaons and antikaons is studied in heavy-ion collisions at CERN SPS and BNL RHIC energies within the microscopic quark–gluon string model. In the midrapidity range the directed flow of kaons v_1 differs considerably from that of antikaons at SPS energy ($E_{\rm lab} = 160\ A$ GeV), while at RHIC energy ($\sqrt{s} = 130\ A$ GeV) the excitation functions of both, kaon and antikaon, flows coincide within the statistical error bars. The change is attributed to formation of dense meson-dominated matter at RHIC, where the differences in interaction cross sections of kaons and antikaons become unimportant. The time evolution of the kaon anisotropic flow is also investigated. The elliptic flow of these hadrons is found to develop at midrapidity at times $3 \leqslant t \leqslant 10$ fm/c, which is much larger than the nuclear passing time $t^{\rm pass} = 0.12$ fm/c. As a function of transverse momentum the elliptic flow increases almost linearly with rising p_t. It stops to rise at $p_t \geqslant 1.5$ GeV/c reaching the saturation value $v_2^K(p_t) \approx 10\%$.

PACS: 25.75.-q; 25.75.Ld; 24.10.Lx

Keywords: Ultrarelativistic heavy-ion collisions; Directed and elliptic flow of kaons; Meson-rich matter; Monte Carlo quark–gluon string model

1. Introduction

The main aim of experiments on heavy-ion collisions at relativistic and ultra-relativistic energies is to study the properties of nuclear matter under extreme conditions and to search for distinct signals from the deconfined quark–gluon plasma (QGP) (see [1] and references therein). The transverse collective flow of particles is at present one of the most intensively studied characteristics of heavy-ion collisions [2–4], because the flow is directly linked to the equation of state (EOS) of the system. If even a small amount of the QGP is formed in the course of the collision, it would lead to a reduction of pressure [5–7] and a softening of the EOS [8,9] that can be detected experimentally. To study the properties of transverse particle flow the method of Fourier series

E-mail address: bravina@th.physik.uni-frankfurt.de (L.V. Bravina).

0370-2693/02
PII: S0370-2693(02)02453-X

expansion [10,11] has been proved to be very useful:

$$E\frac{d^3N}{d^3p} = \frac{d^2N}{2\pi p_t\,dp_t\,dy}\left[1 + 2\sum_{n=1}^{\infty} v_n \cos(n\phi)\right]. \quad (1)$$

Here p_t, y, and ϕ are the transverse momentum, rapidity, and the azimuthal angle of a particle, respectively. The unity in square brackets represents the isotropic radial flow, while the other terms are refer to anisotropic flow. The first Fourier coefficient in Eq. (1) $v_1 = \langle \cos\phi \rangle$ is called directed flow. It represents the averaged ratio of the particle momentum along the impact parameter axis to the transverse momentum, $v_1 = \langle p_x/p_t \rangle$. The second Fourier coefficient $v_2 = \langle \cos(2\phi) \rangle$ is called elliptic flow. It characterizes the eccentricity of the ellipsoid of the particle azimuthal distribution, $v_2 = \langle (p_x/p_t)^2 - (p_y/p_t)^2 \rangle$. Methods proposed for measurement of azimuthal anisotropies in heavy-ion collisions can be found in Refs. [12–14].

The anisotropic flow is a function of rapidity, transverse momentum, and the impact parameter of an event b, i.e., $v_n \equiv v_n(x_j)$, where $\{x_{j=1,2,3}\} \equiv \{y, p_t, b\}$. Therefore, the following differential distributions are usually applied

$$v_n(x_i, \Delta x_{j\neq i}) = \int_{x_j^{(1)}}^{x_j^{(2)}} \cos(n\phi)\frac{d^3N}{d^3x_j}\,d^2x_{j\neq i}\left[\int_{x_j^{(1)}}^{x_j^{(2)}} \frac{d^3N}{d^3x_j}\,d^2x_{j\neq i}\right]^{-1}. \quad (2)$$

The idea that the elliptic flow can carry important information about the early stage of heavy-ion collisions has been discussed already in Ref. [15]. This suggestion is supported by macroscopic hydrodynamic and microscopic transport simulations, which show that elliptic flow saturates quite early [16–20], while directed flow develops almost until the stage of final interactions [21,22]. However, the directed flow of hadrons with high transverse momentum can be used as a probe of hot and dense phase of the collision [23] due to the early freeze-out times of these particles.

In the present Letter we are studying the anisotropic flow of kaons, K^+'s and K^0's, and antikaons, K^-'s and $\overline{K}^0$'s, produced in lead–lead (CERN SPS) and gold–gold (BNL RHIC) collisions at $E_{\rm lab} =$ 160 A GeV and $\sqrt{s} = 130$ A GeV, respectively. Our investigation is inspired by several reasons: First of all, in heavy-ion collisions at GSI SIS (1–2 GeV) and BNL AGS (2–11 A GeV) energies the excitation functions of the directed K^+ and K^- flow are found to be different. At SIS energies the K^+ flow is zero or slightly anticorrelated with the nucleon flow [24,25]. This effect becomes even more pronounced at AGS where a strong anticorrelation between the K^+ and the nucleon flow appears [26]. In both cases, this anticorrelation can be explained by the influence of an in-medium kaon potentials derived from effective chiral models [27]. Kaons experience a weak repulsive potential as a result of superposition of a repulsive vector potential and an attractive scalar potential, whereas antikaons experience a strong attractive potential. Therefore, the directed K^+ flow at these energies is anticorrelated (antiflow) [28,29] while the K^- flow is expected to be similar to the nucleon flow (normal flow) [30].

Does it mean that at energies of SPS and higher, where the mean fields do not play a dominant role, the anisotropic kaon flow would be similar to that of antikaons? Also, multiple particle production at high energies is usually described in the Monte Carlo microscopic models via the formation and break-up of strings stretching between quarks and diquarks (or antiquarks). Kaons, that can be formed on the so-called leading quarks (u and d quarks belonging to primary hadrons), are $K^+(u\bar{s})$ and $K^0(d\bar{s})$ only, but not $K^-(\bar{u}s)$ and $\overline{K}^0(\bar{d}s)$. This may affect the flow of K's, because leading hadrons are carrying larger transverse momenta. Can we see the difference between the coefficients $v_n^{K^+ + K^0}$ and $v_n^{K^- + \overline{K}^0}$ in different rapidity intervals? Finally, K^-'s and $\overline{K}^0$'s can be absorbed via the channels such as $K^- + p \to \Lambda + \pi^+$, etc., whereas there are no analogous reactions for K^+'s and K^0's. How important is this reaction asymmetry at SPS and, especially, at RHIC energies, where the matter is expected to be meson-dominated?

To answer these questions we employed the microscopic cascade quark–gluon string model (QGSM) [31–34]. Description of the model is given in Section 2. Rapidity and transverse momentum dependences of directed (Section 3) and elliptic (Section 4) flow of kaons and antikaons are calculated in Pb + Pb and Au + Au collisions at SPS and RHIC energies,

respectively. Time development of the both flows is studied as well. Finally, conclusions are drawn in Section 5.

2. The model

Similar to the dual parton model (DPM) [35], VENUS [36], and the string fusion model (SFM) [37], QGSM is based on Gribov–Regge theory (GRT) [38] accomplished by a string phenomenology of particle production in inelastic hadron–hadron (hh) collisions. To describe hadron–nucleus and nucleus–nucleus collisions the cascade procedure of multiple secondary interactions of hadrons was implemented. The model incorporates the string fragmentation, formation of resonances, and rescattering of hadrons, but simplifies the nuclear effects neglecting, e.g., the mean fields or evaporation from spectators. As independent degrees of freedom QGSM includes octet and decuplet baryons, octet and nonet vector and pseudoscalar mesons, and their antiparticles. The momenta and positions of nucleons inside the nuclei are generated in accordance with the Fermi momentum distribution and the Woods–Saxon density distribution, respectively. Two particles can interact inelastically with the cross section $\sigma_{\rm inel}(s)$ or elastically with the cross section $\sigma_{\rm el}(s)$ with the "black disk" probability $P(s,b) = \theta(\sigma(s)/\pi - b^2)$. Here $\sigma(s) = \sigma_{\rm inel}(s) + \sigma_{\rm el}(s)$ is the total cross section, b is the impact parameter, and θ is the step function. Pauli blocking of occupied final states is taken into account.

Several different subprocesses are responsible for the string formation in inelastic collisions. A single string can be produced as a result of the valence (di)quark annihilation. This subprocess is important in hh interactions at low energies since the annihilation cross section drops as $s^{-1/2}$. The baryon–antibaryon annihilation in QGSM is modeled via the string junction annihilation with the creation of three strings. In other subprocesses two or more strings can be produced as a result of the colour exchange mechanism, while in single or double diffractive scatterings one or two strings are formed due to momentum transfer. The pomeron, which is a pole with an intercept $\alpha_P(0) > 1$ in the GRT, corresponds to the cylinder-type diagrams. The s-channel discontinuities of the diagrams, representing the exchange by n-pomerons, are related to process of $2k$ ($k \leqslant n$) string production. If the contributions of all n-pomeron exchanges to the forward elastic scattering amplitude are known, the AGK cutting rules [39] enable one to determine the cross sections for $2k$-strings. The hard gluon–gluon scattering and semihard processes with quark and gluon interactions are also incorporated in the model [34]. The inclusive spectra in the QGSM automatically have the correct triple-Regge limit for Feynman variable $x \to 1$, double-Regge limit for $x \to 0$, and satisfy to all conservation laws [31].

Because of the uncertainty principle hadrons produced in string fragmentation can interact further only after a certain formation time. However, hadrons containing the valence quarks of the primary nucleons can interact promptly with reduced interaction cross section. To calculate the statistical weights for the different subprocesses the experimental total, elastic, and inelastic cross sections are used. If the experimental data are lacking, the additive quark model relations, the one-pion exchange model, detailed balance considerations, and isotopic invariance are employed.

The variety of subprocesses included in the model, diagrams with quark annihilation and rearrangement, associated with the exchange of Reggeons, subprocesses with colour exchange which are connected to (multi)pomeron exchanges, as well as hard processes with large momentum transfer, is quite rich. The contribution of each subprocess to the inelastic cross section depends strongly on the bombarding energy. This circumstance enabled the model to predict quantitatively the directed flow of nucleons at SPS [5] more than six years before the first measurements [40,41] and to describe the characteristics of the elliptic flow of charged particles at RHIC [42] measured quite recently [43–45]. The formation of a QGP is not assumed in the present version of the QGSM, although one may consider the strongly interacting field of coloured strings as a precursor of the plasma. Our strategy is to find clear quantitative and qualitative deviations of the experimental results from model predictions. These deviations can then be taken as an indication of new physics, most probably the creation of QGP, not included in the model.

3. Directed flow

Time evolution of directed flow of kaons and antikaons in minimum bias Pb + Pb collisions at 160 A GeV is presented in Fig. 1. Here the coefficient $v_1^K(y)$ is calculated in different transverse momentum intervals at early, $t = 3$ fm/c and $t = 10$ fm/c, and the final stage of the reaction, $t \geqslant 60$ fm/c. To avoid ambiguities, all resonances in the scenario with early freeze-out were allowed to decay according to their branching ratios. The flow evolution is seen quite distinctly. At early stages of the collision directed flow of both kaons and antikaons is oriented in the direction of normal flow similar to that of nucleons [23]. Within the error bars there is no differences between $(K^+ + K^0)$'s and $(K^- + \overline{K}^0)$'s. At this stage the matter is quite dense, mean free paths of particles are short, and similarities in kaon production and rescattering dominate over inequalities caused by different interaction cross sections. It is worth mentioning that the directed flow of K's and $\overline{K}$'s is already sizeable at $t = 3$ fm/c. This can be explained by a kick-off effect associated with the early stage of the collision, when the nuclei pass through each other. Later on the system becomes more dilute. For both kaons and antikaons the directed flow experiences significant transformations as seen in Fig. 1. Already at $t = 10$ fm/c the antiflow of antikaons starts to built up in the midrapidity range. Note, that $t = 10$ fm/c corresponds to the maximum of the kaon dN/dt distribution over their last elastic or inelastic interaction [46]. Here the differences in interaction cross sections and possible reaction mechanisms become crucial. As was found in previous investigations [47,48], particles emitted in the direction of dense baryon-rich matter (i.e., normal flow) will interact more frequently compared to

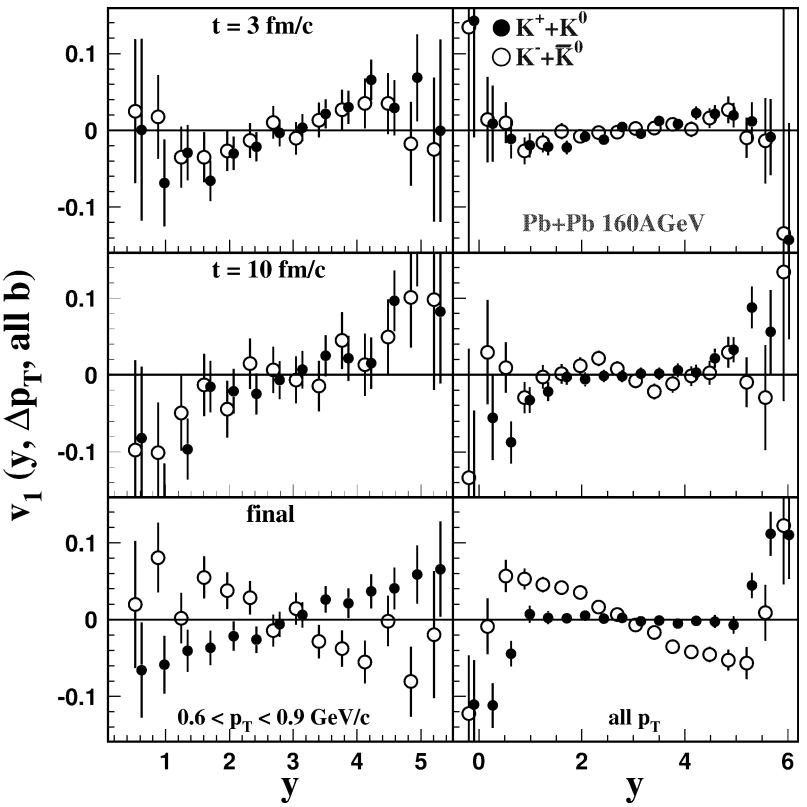

Fig. 1. The directed flow v_1 of kaons (solid circles) and antikaons (open circles) in minimum bias Pb + Pb collisions at SPS energy as a function of rapidity y in high p_t interval $0.6 \leqslant p_t \leqslant 0.9$ GeV/c (left panels) and for all transverse momenta (right panels) at times $t = 3$ fm/c (upper row), 10 fm/c (middle row), and final (bottom row).

those emitted in the opposite, i.e., antiflow, direction. This circumstance reduces the resulting directed flow of kaons almost to zero in a broad midrapidity range. Due to larger interaction cross sections of K^-'s and $\overline{K}^0$'s with other hadrons, the directed flow of these particles changes the orientation from a weak normal to strong antiflow. Even $(K^- + \overline{K}^0)$'s with high transverse momentum demonstrate distinct antiflow, while the flow of $(K^+ + K^0)$'s remains almost unchanged compared to that at $t = 10$ fm/c.

The directed flow of kaons and antikaons in minimum bias Au + Au collisions at $\sqrt{s} = 130$ A GeV is shown in Fig. 2 again at early stages, $t = 3$ fm/c and $t = 10$ fm/c, and at the final one, $t \geqslant 100$ fm/c. It is interesting that at $t = 3$ fm/c (i) the flow of $(K^+ + K^0)$'s coincides within the statistical errors with the $(K^- + \overline{K}^0)$ flow, and (ii) the flow is generally very similar to that at the SPS energy at time $t =$ 3 fm/c. Except of the target and projectile fragmentation region, where again the flow is probably produced by the initial kick, the kaon flow at this early stage of gold–gold collisions at RHIC energy is isotropic with respect to the impact parameter axis. Note that the colliding nuclei have passed through each other already at times less than 0.12 fm/c. The spatial anisotropy in the distribution of baryonic charge seems to be unimportant at this stage. At $t = 10$ fm/c not only the directed flow of antikaons, but also that of kaons becomes antiflow-aligned at midrapidity. Similar behaviour has been found within the RQMD model for the directed flow of nucleons at RHIC [49], suggesting that the nucleon directed flow is a side effect of the elliptic flow. The flow of produced particles, pions [49, 50] and kaons [50], was found to be very flat at $|y| \leqslant 2$, in stark contrast to the QGSM predictions. We are awaiting the experimental data to resolve this problem.

At the final stage of the reaction the excitation functions of both kaon and antikaon flow have a

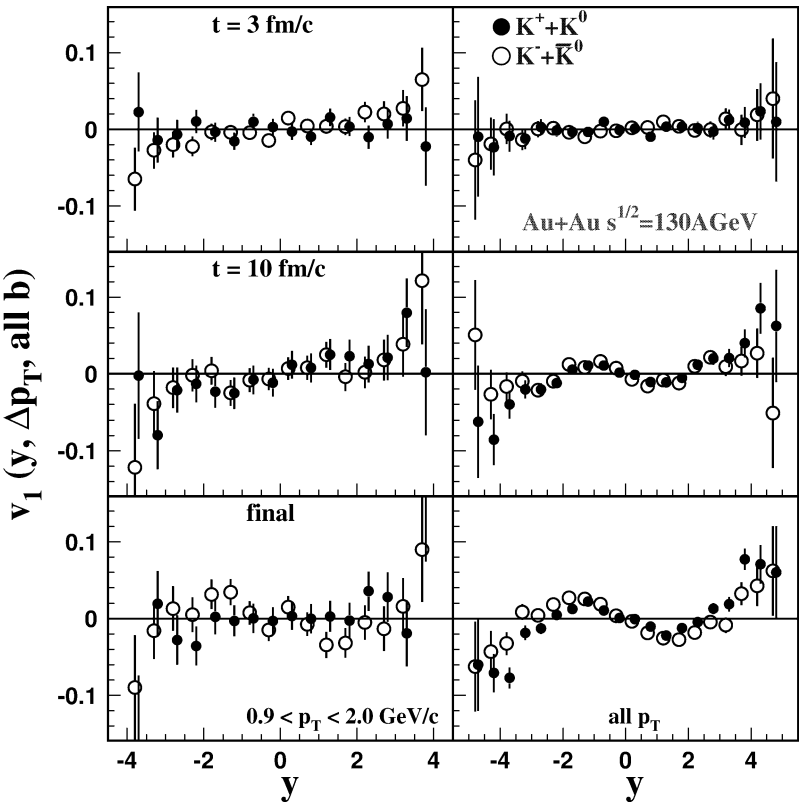

Fig. 2. The same as Fig. 1 but for minimum bias Au + Au collisions at RHIC ($s^{1/2} = 130$ A GeV). For high p_t-kaons transverse momentum varies from 0.9 to 2.0 GeV/c.

similar antiflow behaviour in the midrapidity range compared to the zero flow of $(K^+ + K^0)$'s at lower energies. However, the kaon flow at high transverse momenta $0.9 \leqslant p_t \leqslant 2.0$ GeV/c is elongated in a normal direction. Its slope at the stage of thermal freeze-out is steeper than the slope at $t = 10$ fm/c, i.e., the flow of high p_t-kaons becomes stronger. This means that at RHIC energies the nuclear medium is rather dense, the net baryon density is small, and that kaon–meson (including resonances) reactions dominate over kaon–baryon interactions, which can significantly modify the flow of K^-'s and $\overline{K}^0$'s at SPS energies.

4. Elliptic flow

The study of the development of elliptic flow of kaons in minimum bias Pb + Pb collisions at 160 A GeV, displayed in Fig. 3, reveals that there is no particular direction of kaon emission in the transverse plane at $t = 3$ fm/c. From this time on until the freeze-out stage one cannot distinguish between the elliptic flow of kaons and antikaons in the various p_t-intervals. The resulting elliptic flow of K's and $\overline{K}$'s is positive, i.e., kaons are propagating preferentially in the reaction plane. The flow increases with rising transverse momentum. This behaviour appear to be quite similar to those obtained from the hydrodynamic calculations. Recall that in the hydro models the strong in-plane elliptic flow of hadrons is explained exclusively by the so-called almond shape of the overlapping region of the colliding nuclei. As a consequence of this initial spatial anisotropy, in-plane pressure gradients should be stronger than their out-of-plane counterparts [15]. The fluid acceleration is proportional to the pressure gradient divided by total energy density. During the early stage of the expansion

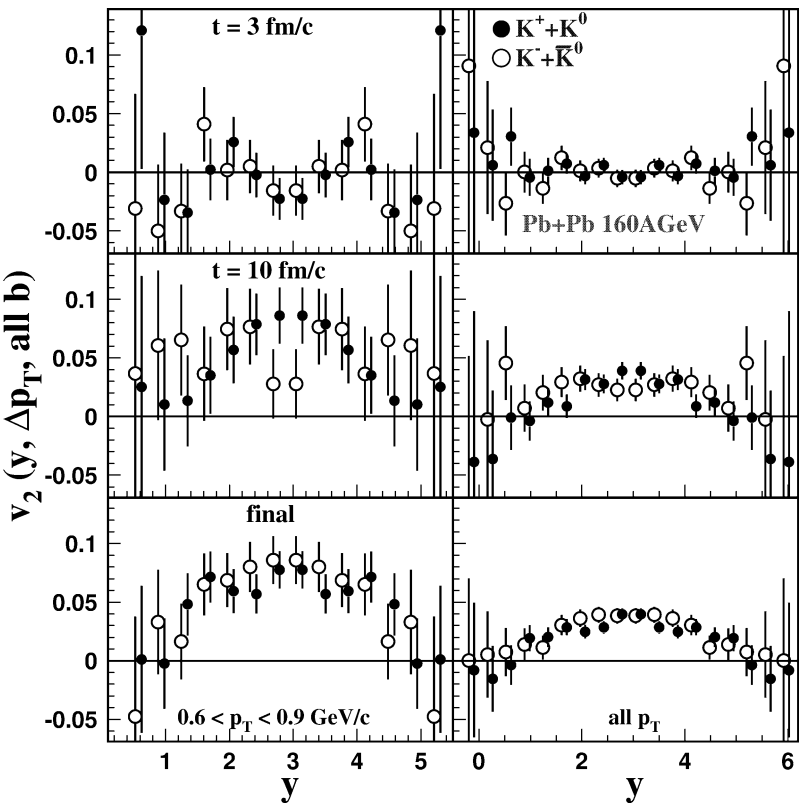

Fig. 3. The same as Fig. 1 but for the elliptic flow v_2 of kaons (solid circles) and antikaons (open circles) in minimum bias Pb + Pb collisions at SPS.

this ratio remains roughly constant. When the spherical shape of the expanding region is restored, the pressure becomes uniform. As was argued in [15], the typical time scale for the transverse flow is the transverse size of the system divided by the sound velocity in the medium. For a semi-peripheral gold–gold or lead–lead collisions this criterion gives us approximately 7 fm/c. At early times the elliptic flow in hydrodynamics increases linearly with time. Therefore, it is quite plausible that the elliptic flow of (anti)kaons at midrapidity in the QGSM calculations is formed within the time interval $3 \leqslant t \leqslant 10$ fm/c in the center-of-mass (CM) system.

Similar features are observed in the development of the elliptic flow of kaons and antikaons in Au + Au collisions at $\sqrt{s} = 130$ A GeV, as one can see in Fig. 4. Their elliptic flow is close to zero in the midrapidity range $|y| \leqslant 2$ at $t = 3$ fm/c. Even the flow of high-p_t particles, which are produced in very energetic hadronic collisions at the beginning of the reaction and which decouple from the system earlier than other particles, shows the same "isotropic" tendency. However, the elliptic flow of kaons and antikaons in the midrapidity range $2 < y < 4$ (SPS) and $|y| \leqslant 1.5$ (RHIC) seems to be formed between 3 and 10 fm/c, i.e., the flow indeed probes the early stage of heavy-ion collisions. The final elliptic flow of both, $(K^+ + K^0)$'s and $(K^- + \overline{K}^0)$'s, is positive in accordance with the predictions of Ref. [15] and its strength increases with rising p_t.

The dip at $y = 0$, clearly seen in Fig. 4, looks a bit peculiar. However, the signal is not unique. The appearance of similar midrapidity dip in the $v_2(y)$ distribution of hadrons, calculated in [50] at full RHIC energy $\sqrt{s} = 200$ A GeV within the UrQMD model, is linked to the particle formation time. Our study supports this conclusion. Fig. 4 shows that the effect is stronger for high-p_t kaons, which have longer

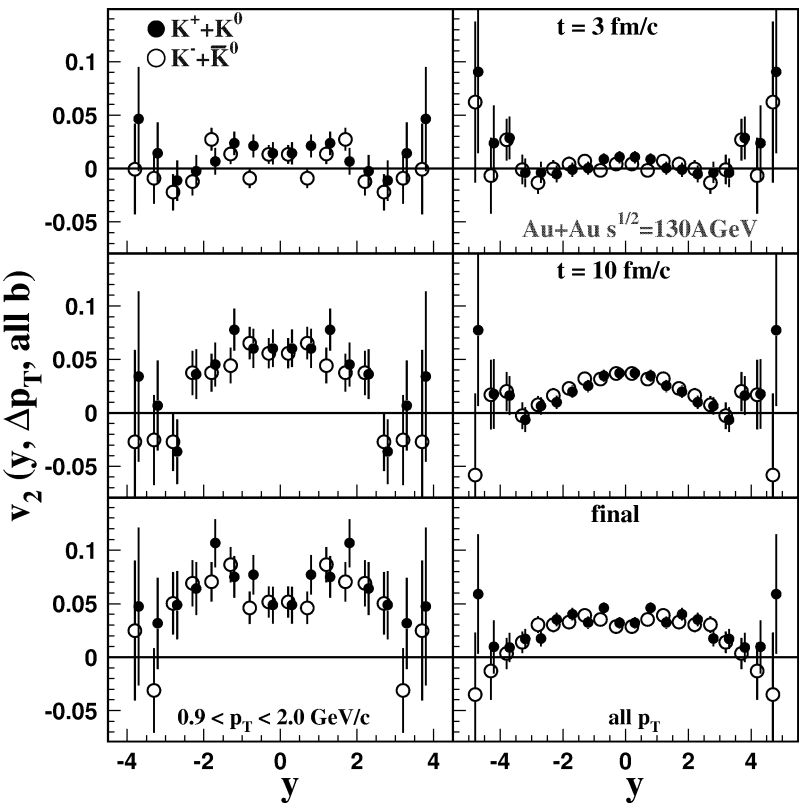

Fig. 4. The same as Fig. 2 but for the elliptic flow v_2 of kaons (solid circles) and antikaons (open circles) in minimum bias Au + Au collisions at RHIC.

formation time due to higher momentum. Shorter formation times lead to increase of the elliptic flow, and the dip vanishes.

The transverse momentum dependence of the elliptic flow in both reactions is presented in Fig. 5. Again, in the very early phase of the collision the flow $v_2^{K(\overline{K})}(p_t)$ is absent. At time $t = 10$ fm/c the elliptic flow of kaons and antikaons seems to be already formed. It is close to zero for kaons and antikaons with low transverse momenta, $p_t \leqslant 0.25$ GeV/c, and then rises linearly up to $v_2^K(p_t) \approx 10\%$ within the interval $0.25 \leqslant p_t \leqslant 1.5$ GeV/c. At transverse momenta higher than 1.5 GeV/c the elliptic flow saturates in accord with experimental results [51]. Note, that if the hydrodynamic regime would be reached, the excitation function of the elliptic flow $v_2^K(p_t)$ should grow further almost linearly above $p_t \geqslant 1.5$ GeV/c also [17].

The delay in the development of the elliptic flow and the saturation of the flow after a certain p_t-limit can be explained as follows. The bulk production of new particles takes place within the first few fm/c's, when parton and hadron collisions are extremely energetic. Kaons, as well as other hadrons produced as a result of string fragmentation, are emitted isotropically in the azimuthal plane. To develop the anisotropic flow these hadrons have to rescatter in a spatially anisotropic nuclear matter. But because of the uncertainty principle the only particles allowed to interact immediately (although with reduced cross sections) are those containing the valence quarks. For all other hadrons a proper formation time should pass between the rescatterings. Due to the finiteness of colliding nuclei, there is a saturation of number of secondary interactions per hadron with the transverse momentum higher than certain

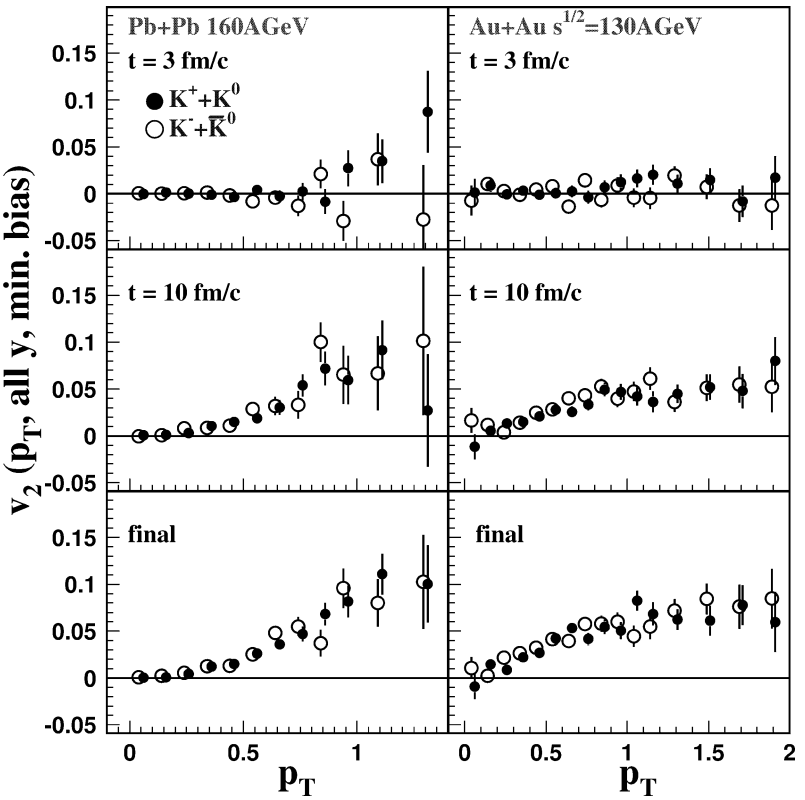

Fig. 5. Transverse momentum dependence of the elliptic flow of kaons (solid circles) and antikaons (open circles) in minimum bias Pb + Pb collisions at SPS (left panels) and Au + Au collisions at RHIC (right panels) at early times $t = 3$ fm/c (upper row), 10 fm/c (middle row), and freeze-out times (bottom row) of the reaction.

p_t. Therefore, the elliptic flow of high-p_t particles also saturates. Here it is worth to mention that the problem of the formation time of hadrons produced in a very dense and hot nuclear medium, which is formed in heavy-ion collisions at energies of RHIC and higher, is studied insufficiently. A shorter formation time will reduce the mean free path of particles, thus increasing the collision rates and enhancing the elliptic flow. This can be the reason why the plateau in the excitation function $v_2^{K(\overline{K})}(p_t)$, predicted by the QGSM (see Fig. 5), is a bit lower compared to the data. This question should be clarified in nearest future.

5. Discussion and conclusions

In summary, the anisotropic flow of kaons and antikaons is studied in lead–lead and gold–gold collisions at SPS and RHIC energies, respectively, within the microscopic cascade quark–gluon string model. The directed flow of kaons $v_1^{K^+ + K^0}(y, \Delta p_t)$ at SPS energy is close to zero in a broad rapidity range except of the projectile and target fragmentation regions, while the directed flow of antikaons $v_1^{K^- + \overline{K}^0}(y, \Delta p_t)$ has a linear antiflow slope. At early times $t \leqslant 3$ fm/c for both particle species the directed flow is oriented in the direction of normal flow. The difference in final distributions is attributed to the different interaction cross sections with the surrounding nuclear matter and to the large absorption cross section of antikaons with baryons. In heavy-ion collisions at RHIC energies a dense meson-dominated matter with low net baryon density is formed. Hence, the directed flow of kaons becomes similar to that of antikaons, i.e., in both cases the flow is elongated in antiflow direction at $|y| \leqslant 2$ and in normal flow direction at higher rapidity, $|y| \geqslant 2$. The predicted antiflow of K's in the central rapidity range is an order of magnitude stronger compared to the signal predicted by the UrQMD model. These are the main results of our study. Since the differences between the functions $v_1^{K^+ + K^0}(y)$ and $v_1^{K^- + \overline{K}^0}(y)$ in the fragmentation regions in different transverse momentum intervals are found to be within the statistical error bars, we conclude that the formation of fast kaons on leading u and d quarks plays only a minor role at RHIC energies.

The elliptic flow of both kaons and antikaons in the midrapidity range is built up at times between 3 and 10 fm/c, although the passing time even for central heavy-ion collisions is 1.44 fm/c and 0.12 fm/c at SPS and RHIC energy, respectively. In contrast to the midrapidity range, the elliptic flow of kaons and antikaons with rapidity $y \geqslant 1.5$ continues to develop after $t = 10$ fm/c in the center-of-mass system. The rapidity distribution of the function $v_2^{K(\overline{K})}$ is flat over a broad range $|y| \leqslant 3$ at RHIC energies. As a function of transverse momentum the elliptic flow of K's and $\overline{K}$'s rises linearly with increasing p_t and saturates at $p_t \geqslant 1.5$ GeV/c. The plateau at high transverse momenta can be explained by saturation of number of secondary interactions experienced by hadrons with a transverse momentum higher than a certain limiting value.

Acknowledgements

Fruitful discussions with Yu. Dokshitzer, J.-Y. Ollitrault, S. Panitkin, D. Röhrich, D. Strottman, and N. Xu are gratefully acknowledged. This work was supported in part by the Bundesministerium für Bildung und Forschung (BMBF) under contract 06TÜ986, and by the Bergen Computational Physics Laboratory (BCPL) in the framework of the European Community—Access to Research Infrastructure action of the Improving Human Potential Programme.

References

[1] Proceedings of the QM'2001 Conference, Nucl. Phys. A 698 (2002).
[2] W. Reisdorf, H.G. Ritter, Annu. Rev. Nucl. Part. Sci. 47 (1997) 663.
[3] N. Herrmann, J.P. Wessels, T. Wienold, Annu. Rev. Nucl. Part. Sci. 49 (1999) 581.
[4] J.-Y. Ollitrault, Nucl. Phys. A 638 (1998) 195c.
[5] N.S. Amelin, et al., Phys. Rev. Lett. 67 (1991) 1523.
[6] L.V. Bravina, L.P. Csernai, P. Levai, D. Strottman, Phys. Rev. C 50 (1994) 2161.
[7] L.P. Csernai, D. Röhrich, Phys. Lett. B 458 (1999) 454.
[8] C.M. Hung, E.V. Shuryak, Phys. Rev. Lett. 75 (1995) 4003.
[9] D.H. Rischke, M. Gyulassy, Nucl. Phys. A 597 (1996) 701.
[10] S. Voloshin, Y. Zhang, Z. Phys. C 70 (1996) 665.
[11] A.M. Poskanzer, S.A. Voloshin, Phys. Rev. C 58 (1998) 1671.
[12] P. Danielewicz, G. Odyniec, Phys. Lett. B 157 (1985) 146.

[13] N. Borghini, P.M. Dinh, J.-Y. Ollitrault, Phys. Rev. C 63 (2001) 054906;
N. Borghini, P.M. Dinh, J.-Y. Ollitrault, Phys. Rev. C 64 (2001) 054901.
[14] N. Borghini, et al., Phys. Rev. C 66 (2002) 014901.
[15] J.-Y. Ollitrault, Phys. Rev. D 46 (1992) 229;
J.-Y. Ollitrault, Phys. Rev. D 48 (1993) 1132.
[16] H. Sorge, Phys. Rev. Lett. 78 (1997) 2309.
[17] P.F. Kolb, J. Sollfrank, U. Heinz, Phys. Lett. B 459 (1999) 667;
P.F. Kolb, P. Huovinen, U. Heinz, H. Heiselberg, Phys. Lett. B 500 (2001) 232.
[18] H. Heisenberg, A.-M. Levy, Phys. Rev. C 59 (1999) 2716.
[19] B. Zhang, M. Gyulassy, C.M. Ko, Phys. Lett. B 455 (1999) 45.
[20] D. Molnar, M. Gyulassy, Nucl. Phys. A 698 (2002) 379c, nucl-th/0104073.
[21] H. Liu, S. Panitkin, N. Xu, Phys. Rev. C 59 (1999) 348.
[22] J. Brachmann, et al., Phys. Rev. C 61 (2000) 024909.
[23] E.E. Zabrodin, C. Fuchs, L.V. Bravina, A. Faessler, Phys. Rev. C 63 (2001) 034902.
[24] J.L. Ritman, et al., FOPI Collaboration, Z. Phys. A 352 (1995) 355.
[25] Y. Shin, et al., KaoS Collaboration, Phys. Rev. Lett. 81 (1998) 1576.
[26] P. Chung, et al., E895 Collaboration, Phys. Rev. Lett. 85 (2000) 940.
[27] D.B. Kaplan, A.E. Nelson, Phys. Lett. B 175 (1986) 57.
[28] C.Q. Li, C.M. Ko, B.A. Li, Phys. Rev. Lett. 74 (1995) 235;
G.Q. Li, C.M. Ko, Nucl. Phys. A 594 (1995) 460;
Z.S. Wang, et al., Nucl. Phys. A 628 (1998) 151;
C. Fuchs, et al., Phys. Lett. B 434 (1998) 245.
[29] S. Pal, C.M. Ko, Z. Lin, B. Zhang, Phys. Rev. C 62 (2000) 061903(R).
[30] G. Song, B.A. Li, C.M. Ko, Nucl. Phys. A 646 (1999) 481.
[31] A.B. Kaidalov, Phys. Lett. B 116 (1982) 459;
A.B. Kaidalov, K.A. Ter-Martirosian, Phys. Lett. B 117 (1982) 247.
[32] N.S. Amelin, L.V. Bravina, L.I. Sarycheva, L.N. Smirnova, Sov. J. Nucl. Phys. 50 (1989) 1058;
N.S. Amelin, L.V. Bravina, Sov. J. Nucl. Phys. 51 (1990) 133.
[33] N.S. Amelin, et al., Phys. Rev. C 47 (1993) 2299.
[34] N.S. Amelin, E.F. Staubo, L.P. Csernai, Phys. Rev. D 46 (1992) 4873.
[35] A. Capella, U. Sukhatme, C.I. Tan, J. Tran Thanh Van, Phys. Rep. 236 (1994) 225.
[36] K. Werner, Phys. Rep. 232 (1993) 87.
[37] N.S. Amelin, M.A. Braun, C. Pajares, Phys. Lett. B 306 (1993) 312;
N.S. Amelin, N. Armesto, C. Pajares, D. Sousa, Eur. Phys. J. C 22 (2001) 149.
[38] V. Gribov, Sov. Phys. JETP 26 (1968) 414;
L.V. Gribov, E.M. Levin, M.G. Ryskin, Phys. Rep. 100 (1983) 1.
[39] V. Abramovskii, V. Gribov, O. Kancheli, Sov. J. Nucl. Phys. 18 (1974) 308.
[40] H. Appelshäuser, et al., NA49 Collaboration, Phys. Rev. Lett. 80 (1998) 4136.
[41] M.M. Aggarwal, et al., WA98 Collaboration, Phys. Lett. B 469 (1999) 30.
[42] E.E. Zabrodin, C. Fuchs, L.V. Bravina, A. Faessler, Phys. Lett. B 508 (2001) 184.
[43] STAR Collaboration, K.H. Ackermann, et al., Phys. Rev. Lett. 86 (2001) 402.
[44] I.C. Park, PHOBOS Collaboration, Nucl. Phys. A 698 (2002) 564c.
[45] R. Lacey, PHENIX Collaboration, Nucl. Phys. A 698 (2002) 559c.
[46] L.V. Bravina, et al., Phys. Rev. C 60 (1999) 044905.
[47] L.V. Bravina, Phys. Lett. B 344 (1995) 49.
[48] L.V. Bravina, E.E. Zabrodin, A. Faessler, C. Fuchs, Phys. Lett. B 470 (1999) 27;
L.V. Bravina, A. Faessler, C. Fuchs, E.E. Zabrodin, Phys. Rev. C 61 (2000) 064902.
[49] R.J.M. Snellings, Phys. Rev. Lett. 84 (2000) 2803.
[50] M. Bleicher, H. Stöcker, Phys. Lett. B 526 (2002) 309.
[51] R.J.M. Snellings, STAR Collaboration, Nucl. Phys. A 698 (2002) 193c.